JOURNAL OF MATERIALS SCIENCE 28 (1993) 2639–2653

Si–C–N ceramics with a high microstructural stability elaborated from the pyrolysis of new polycarbosilazane precursors

Part III *Effect of pyrolysis conditions on the nature and properties of oxygen-cured derived monofilaments*

D. MOCAER, R. PAILLER, R. NASLAIN
Laboratoire des Composites Thermostructuraux (UMR-47 CNRS-SEP-UB1), Domaine Universitaire, 3 allée de La Boëtie, F-33600-Pessac, France

C. RICHARD, J. P. PILLOT, J. DUNOGUES
Laboratoire de Chimie Organique et Organométallique (URA 35-CNRS), Université Bordeaux-I, 351 Cours de la Libération, F-33405-Talence, France

O. DELVERDIER, M. MONTHIOUX
Laboratoire Marcel Mathieu (UMR-CNRS-DRET), 2 Avenue Président Pierre Angot, F-64000 Pau, France

Melt-spun/oxygen-cured polycarbosilazane monofilaments were pyrolysed under an argon or nitrogen atmosphere at pyrolysis temperatures, θ_p, up to 1600 °C. The organic/inorganic transition took place at $500 < \theta_p < 850$ °C with a first weight loss and diameter shrinkage (evolution of CH_4 and H_2). It yielded an amorphous Si–C–N–O material which underwent only minor changes (e.g. densification) when θ_p was raised to about 1400 °C. In contrast, beyond 1400 °C, major changes occurred which depended on the pyrolysis atmosphere. Under argon, a decomposition/crystallization process yielded a second weight loss and diameter shrinkage (evolution of SiO, CO, N_2) and resulted in a β-SiC + C mixture whose degree of crystallization increased when θ_p was raised. Under nitrogen, a decomposition/nitriding process yielded a material enriched in nitrogen and depleted in oxygen which remained partially amorphous up to 1600 °C. The tensile failure stress at room temperature increased sharply for $500 < \theta_p < 800$ °C and reached a maximum (close to 2000 MPa) for $\theta_p = 1200$ °C whereas the Young's modulus increased more smoothly with a maximum (close to 175 GPa) for $\theta_p \approx 1400$ °C. Both oxygen and nitrogen have an impeding effect on the crystallization of β-SiC. Thus, the best mechanical properties were obtained for filaments pyrolysed under nitrogen. A semi-conducting/semi-metallic transition was observed for $\theta_p \approx 1400$ °C related to the decomposition of the amorphous Si–C–N–O material and formation of free carbon. Ex-polycarbosilazane oxygen-cured filaments exhibited a thermal stability somewhat higher than their ex-polycarbosilazane counterparts.

1. Introduction

During the last decade, various Si–C–O, Si–N–O, Si–C–Ti–O and Si–C–N–O ceramic fibres have been produced from organosilicon polymeric precursors, using a general process involving: (i) spinning of the precursor usually in the molten state, (ii) a curing step performed under air or oxygen and (iii) a pyrolysis at high temperatures under an inert atmosphere [1–7].

Most of the Si–C–O fibres described in the literature derived from the pioneering work of Yajima and co-workers [1–3]. Some of them (Nicalon fibres, standard and ceramic grades, from Nippon Carbon) are commercially available and commonly used as reinforcements in ceramic matrix composites (CMC). These fibres are prepared from polycarbosilane (PCS) precursors. In the as-prepared state, the fibres exhibit a complex composition which can be described, on the basis of the most recent analyses as a mixture of β-SiC nanocrystals, an amorphous SiC_xO_y phase (in which silicon is tetrahedrally coordinated to carbon and oxygen atoms: $x + y = 4$) and finally, free carbon present at the nanometre scale as basic structural units (BSU) [8–10]. Depending on the processing conditions, the relative amounts of the β-SiC and amorphous SiC_xO_y phases are different and the BSUs more or less well arranged with respect to each other and to the other phases (in some cases, the BSUs were observed to form cage-like structures around the β-SiC nanocrystals) [7]. Ex-PCS Si–C–O fibres exhibit at room temperature a Young's modulus of about 180 GPa (i.e.

0022–2461

$140 < E < 220$ GPa) and a failure tensile stress which can be as high as 3500 MPa for the best materials. Unfortunately, these mechanical properties decrease in a dramatic manner when the fibres have been aged (under vacuum or inert atmosphere) above about 1200 °C, due to the decomposition of SiC_xO_y amorphous phase (which yields an evolution of SiO and CO) and simultaneously a coarsening of the β-SiC phase [7, 11].

Si–N–O fibres have been prepared by Okamura and co-workers according to a related procedure: after spinning, oxygen-curing and pyrolysis performed at $1000 < \theta_p < 1650$ °C (where θ_p is the pyrolysis temperature, under pure nitrogen) the fibres are submitted to a post-treatment at $\theta > 800$ °C under an atmosphere of ammonia in order to replace the carbon present in the fibre by nitrogen [12, 13]. The resulting Si–N–O fibres were reported to have a better thermal stability. Their failure tensile stress at room temperature, is maximum (1750 MPa) when $\theta_p = 1300$ °C and it is still significant (1300 MPa) when θ_p is raised up to 1400 °C.

Si–C–Ti–O fibres have been prepared according to a process deriving from the Yajima route, utilizing a polytitanocarbosilane (PTCS) as the starting polymeric material [14, 15]. The resulting fibres, now commercially available (Tyranno fibres), are smaller in diameter than their Si–C–O counterpart (i.e. 8 μm compared to 15 μm) but their mechanical properties at room temperature ($E = 180$ GPa) and $\sigma^R = 3000$ MPa for $\theta_p \approx 1300$ °C) are very similar. Their overall chemical formula is close to $SiC_{1.32}O_{0.96}Ti_{0.04}$ and they are mainly amorphous [16]. When aged above 1300 °C, Si–C–Ti–O fibres undergo a decomposition process yielding various crystalline phases (i.e. mainly β-SiC and TiC) [16, 17] and a dramatic decrease in their mechanical properties [3, 18].

Quaternary Si–C–N–O fibres have been prepared, from different organosilicon precursors, according to the spinning/oxygen-curing/pyrolysis route. Penn *et al.* [19, 20] following the early work of Verbeek [21], have described the preparation of such fibres from a polycarbosilazane (PCSZ) precursor which contained polysilazane cycles bonded together through the polycondensation of *tris* (*N*-methylamino) methylsilane and *tris* (*N*-methylamino) phenylsilane monomers. After spinning, the green fibres were cured with water vapour and pyrolysed at $\theta_p = 1200$–1500 °C under nitrogen. The resulting Si–C–N–O fibres (13 μm diameter) were reported to exhibit a Young's modulus of 200 GPa and a tensile failure stress of 1000 MPa at room temperature, as well as a good microstructural stability after ageing in air at temperature up to 1200 °C.

More recently, two new Si–C–N–O fibres have been elaborated from a phenylvinyl silazane containing 20 mol% methyl-polydisilazane precursor (MPDZ fibres, Dow-Corning), on the one hand, and a polysilazane precursor (Fiberamic fibres, Rhône Poulenc), on the other hand [22–24]. The former was reported to be characterized by an overall formula $SiC_{1.4}N_{0.6}O_{0.3}$, a diameter ranging from 10–15 μm, a density of 2.3 g cm^{-3}, a tensile failure stress of 1900 MPa and a stiffness of 190 GPa at room temperature [22, 23] and the latter by an overall formula $SiC_{0.53}N_{0.77}O_{0.25}$, an average diameter of 15 μm, a density of 2.3 g cm^{-3}, $\sigma^R = 2000$ MPa and $E = 200$ GPa [25]. It is worthy of note that all the Si–C–N–O fibres are amorphous (on the basis of their X-ray diffraction pattern) and exhibit an improved thermal stability (with respect to their Si–C–O counterparts).

The present work is part of a more general study devoted to Si–C–N (or Si–C–N–O) ceramics deriving from a new polycarbosilazane precursor prepared according to a copolycondensation/thermal rearrangement process, from dimethyldichlorosilane and 1,3-dimethyl 1,3-dichlorodisilazane taken in an equimolar ratio [26]. This PCSZ precursor has been spun at the molten state in order to yield a continuous green model filament whose curing by oxygen has been studied in detail elsewhere [27]. The aim of the present work was: (i) to study the variation of the properties of the monofilament as a function of the pyrolysis conditions (namely temperature and atmosphere) and (ii) to derive correlations between these properties, and monofilament composition and microstructure.

2. Experimental procedure

2.1. The ex-PCSZ Si–C–N–O monofilament

The PCSZ-precursor used in this study was prepared according to a two-step procedure, which has been described in detail elsewhere [26]. In a first step, a polysilasilazane (PSSZ) was prepared by adding both dimethyldichlorosilane and 1,3-dichloro 1,3-dimethyldisilazane in a molar ratio of 1 to a suspension of sodium in boiling toluene. The PSSZ was converted in a second step into PCSZ in a fluidized bed heated at 400–425 °C. The precursor used in the present study is that referred to PCSZ-II in Part 1, its overall chemical composition corresponds to the formula $SiC_{1.22}N_{0.45}H_{4.2}O_{0.03}$ [28]. PCSZ-II was spun at the molten state, with a single spinneret apparatus, a mechanical stretching being applied to the filament, through the take-up reel, in order to achieve an average diameter of 25 μm.

The green continuous PCSZ monofilament was cut as samples of length $L = 50$ mm and then chemically cured. The curing process was performed under an atmosphere of a mixture of pure oxygen ($P = 50$ kPa) and pure nitrogen ($P = 50$ kPa) [27]. The samples, set in a boat of silica, were first progressively heated up to 190 °C (ramping temperature 5 °C h^{-1}) and maintained at this temperature for 1 h.

The oxygen-cured PCSZ filaments were finally converted into Si–C–N–O ceramic filaments according to a two-step pyrolysis procedure. First, the PCSZ filaments were heated under a stream of pure argon ($P = 100$ kPa; gas flow rate 1 l h^{-1}) up to $\theta_p = 700$–850 °C and maintained at this temperature for 15 min. In a second step, the pre-pyrolysed samples were heated under an argon or nitrogen atmosphere ($P = 100$ kPa; gas flow rate 1–2 l h^{-1}) up to a temperature θ_p ranging from 1200–1600 °C and maintained at θ_p for 15 min. The resulting Si–C–N–O ceramic

monofilaments have a diameter of the order of 20 μm. Owing to the aim of the present study, they were regarded as model materials and therefore, no attempt was made to reduce their diameter in order to improve, for example, their tensile failure stress, as already mentioned.

2.2. Physico-chemical characterization

TGA experiments were performed with an apparatus (TAG 24 from SETARAM) constituted with graphite furnace and crucible, up to 1600 °C under an argon or nitrogen atmosphere (P = 100 kPa; ramping temperature 600 °C h^{-1}).

Analysis of the gaseous species formed during the pyrolysis, was performed according to two different procedures, i.e. by chromatography or high-resolution mass spectroscopy (VG 7070 F mass spectrometer, in order to analyse both CO and N_2), described elsewhere [28].

The elemental composition of the Si–C–N–O samples was assessed, from polished metallographic cross sections, by electron probe microanalysis (EPMA, CAMEBAX 75, CAMECA) utilizing two different monochromators (i.e. a PET crystal for SiK_α and a multilayer pseudo crystal PCI for CK_α, NK_α and OK_α) and standards of pure SiC, BN and SiO_2. Hydrogen, which cannot be analysed by EPMA, was not determined, although it has been shown to be present in small amounts in the pyrolytic residues of PCSZ at least for low θ_p values [28].

Auger electron spectroscopy (AES) characterization was performed with a scanning microprobe (PHI 5905 AM from Perkin–Elmer) equipped with an Ar^+ sputtering gun. The variations of the intensities of the Auger electron peaks (Si-*LVV*, C-*KLL*, N-*KLL* and O-*KLL*) as a function of the sputtering time were used to draw semi-quantitatively composition–depth profiles from sample surface.

X-ray diffraction (XRD) patterns were recorded with a powder diffractometer (CuK_α wavelength) (PW 1710 deffractometer, Philips) from monofilaments which were ground with an agate mortar.

The structure of the monofilaments was studied at the nanometre scale by high-resolution transmission electron microscopy (TEM, Philips EM 400). Each sample was embedded in an epoxy resin and thin foils were prepared by ultramicrotomy, according to the procedure described by Maniette and Oberlin [29]. The TEM analyses were performed in the bright-field, dark-field and selected-area diffraction (SAD) modes [30]. The apparent diameter of the aperture in the Abbe plan of the objective lens of the microscope was 1.9 nm^{-1} in the dark-field imaging mode. Two aperture positions were used: in position 1, the aperture was centred at 2.4 nm^{-1} and its diameter admitted among others the 0 0 2 reflection of carbon (and possibly the most intense halo of amorphous SiO_2), whereas in position 2, it was centred at 4.2 nm^{-1} and selected among others the 1 1 1 reflection of β-SiC (blende type) [31].

Density was measured with an helium pycnometer on 100–200 mg samples with an accuracy of the order of 5%. Finally, the electrical conductivity measurements were performed, according to the four-point method from room temperature to 600 °C, on tows of about ten monofilaments. Because the PCSZ pyrolytic residues usually behave as semi-conducting materials, the resulting data were used to draw $\log_{10}\sigma = f(1/T)$ plots (where σ and T are the electrical conductivity and the temperature in Kelvin at which it was measured, respectively) in order to calculate the related apparent activation energies, E_a.

2.3. Mechanical tensile tests

The Si–C–N–O monofilaments were tested in tension, at room temperature, with an apparatus similar to that described by Bunsell *et al.* (gauge length L = 10 mm) [32]. For each pyrolysis temperature value, θ_p, an average of 20 tests were performed in order to calculate the average tensile failure stress σ^R and Young's modulus, E.

3. Results

3.1. Weight loss and gas evolution during pyrolysis

As shown in Fig. 1, three successive weight losses occur when a sample of oxygen-cured PCSZ monofilaments is progressively heated under an argon or nitrogen atmosphere. Under argon the first weight loss, which takes place between 25 and 500 °C, is very limited in magnitude (i.e. of the order of 2%); the second, occurring between 500 and 900 °C, is more significant (about 10%), and the third, which is also the most important (about 44%), is observed beyond 1400 °C. Thus it appears that the material remains stable, as far as weight loss is concerned within a rather broad temperature range (i.e. from 900–1400 °C). Under a nitrogen atmosphere the weight loss below 1400 °C is similar to that under argon. On the contrary, between 1400 and 1500 °C, the weight loss is about nil, whereas between 1500 and 1600 °C the weight loss occurring is about 12%.

On the basis of our previously published results on the pyrolysis of bulk PCSZ samples [28], the weight loss occurring at 500–900 °C can be assigned to the organic/inorganic transition which is known to yield an evolution of various gases including CH_4 and hydrogen as the main ones.

On the basis of the gas analysis data shown in Fig. 2, the most important weight loss occurring beyond 1400 °C can be assigned mainly to an evolution of carbon monoxide, nitrogen and hydrogen to a less extent. Fig. 2a shows the gas evolution under vacuum from a Si–C–N–O filament sample, which has been first pyrolysed up to 1200 °C (according to the two-step procedure described in Section 2.1), as the temperature is raised from 1200 °C to 1600 °C. The evolution of CO becomes noticeable under vacuum at 1200 °C, but it remains slow up to 1400 °C. At that temperature, it dramatically increases and the evolution of nitrogen simultaneously starts.

As previously mentioned, the pyrolytic residues resulting from the organic/inorganic transition taking

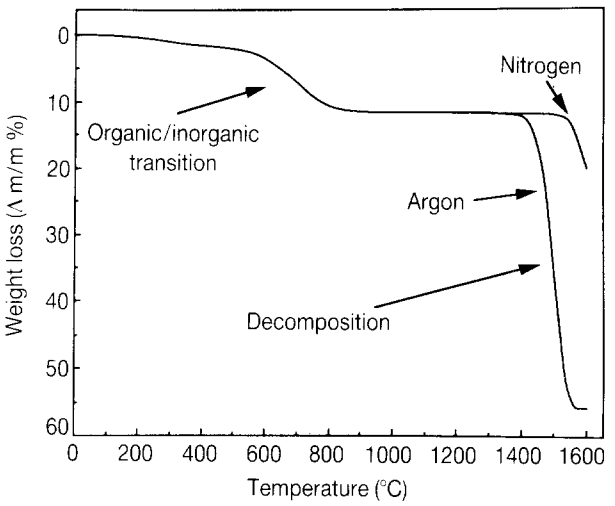

Figure 1 Weight loss occurring during the pyrolysis of oxygen-cured PCSZ monofilaments, under an argon or nitrogen atmosphere (P = 100 kPa; Q = 1 l h^{-1}).

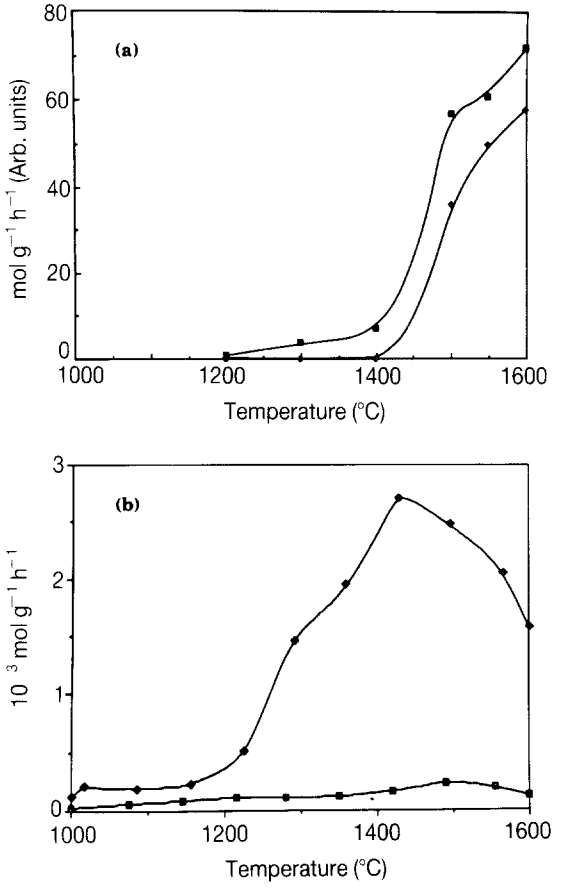

Figure 2 Gas evolution during the pyrolysis of the ex-PCSZ filaments: (a) evolution of (■) CO and (◆) nitrogen under vacuum as established by high-resolution mass spectroscopy for filaments which have been first prepyrolysed up to 1200 °C under an inert atmosphere, (b) evolution of hydrogen under a flow of purified nitrogen as established by gas chromatography for (■) an oxygen-cured filament sample and (◆) an uncured PCSZ.

place in bulk PCSZ samples are known to contain small amounts of hydrogen [28]. This is also true for the Si–C–N–O filaments resulting from the pyrolysis of oxygen-cured PCSZ green filaments, as shown by the evolution of hydrogen observed in the 1000–1600 °C temperature range (Fig. 2b). It is noteworthy that the evolution of hydrogen occurring after the organic/inorganic transition (i) undergoes a maximum at a surprisingly high temperature (i.e. 1450–1500 °C), and (ii) is less significant for the oxygen-cured PCSZ filaments than for an uncured similar PCSZ sample.

TABLE I Chemical composition (as established from EPMA analyses) of Si–C–N–O monofilaments spun from PCSZ molten precursor, cured in oxygen and pyrolysed under various conditions (hydrogen is not detected by EPMA)

Pyrolysis atmosphere	Temperature θ_p(°C)	Si (at %)	C (at %)	O (at %)	N (at %)
	1000	36	29	21	14
	1200	36	28	22	14
argon					
	1400	35	29	20	14
	1600	43	56	0.5	0.5
	1200	36	28	22	14
	1400	36	28	22	14
nitrogen					
	1500	36	27	21	16
	1600	36	31	7	26

3.2. Chemical composition of the filaments as a function of θ_p

The results of the elemental chemical analyses performed by EPMA (and thus neglecting hydrogen) on ex-PCSZ Si–C–N–O filaments pyrolysed at increasing θ_p, are shown in Table I. For θ_p values ranging from the organic/inorganic transition up to 1400 °C, the elemental composition of the filament core remains almost unchanged (neglecting hydrogen). Because the initial PCSZ precursor was almost free of oxygen (as mentioned in Section 2.1), the data suggest that the curing process is mainly responsible for the 20 at % oxygen present in the ceramic filament, the oxygen contamination during pyrolysis being of the order of 1–3 at %, as established previously from the pyrolysis of uncured bulk PCSZ samples [28]. The overall chemical composition of the Si–C–N–O filaments corresponds closely to the formula $SiC_{0.78}N_{0.39}O_{0.61}$. On the other hand, it clearly appears that for $\theta_p > 1400$ °C the filament composition depends on the nature of the atmosphere flowing in the pyrolysis furnace. When the pyrolysis has been performed under argon at 1600 °C, the filament is almost totally free of both oxygen and nitrogen and it contains only silicon and carbon (with a C/Si atomic ratio higher than unity). Otherwise, when it has been performed under nitrogen, the data show that the atomic concentration in nitrogen increases from 14% to 26%, whereas simultaneously that in oxygen decreases from 22% to 7%, as θ_p is raised from 1400 °C to 1600 °C (the C/Si atomic ratio remaining almost unchanged and close to unity).

The evolution of CO and N_2 observed under vacuum beyond 1400 °C together with the elemental composition data, suggested that a decomposition process occurs in the Si–C–N–O filaments at very high temperatures, moving possibly from the external surface towards the core. AES depth profile analyses were performed starting from the filament surface, in

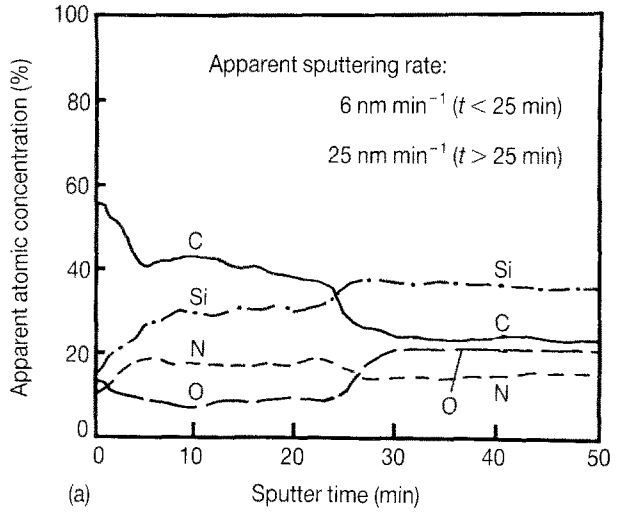

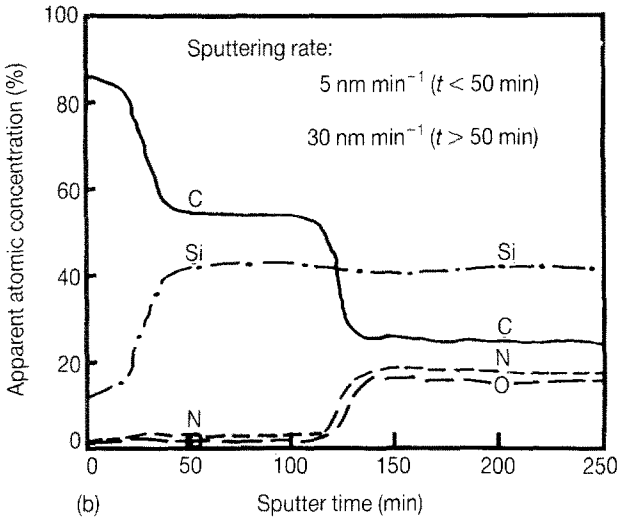

Figure 3 AES depth profile analyses near the filament external surface recorded for Si–C–N–O filaments pyrolysed under a gas flow of argon ($P = 100$ kPa; $Q = 1\,l\,h^{-1}$) during 15 min: (a) at $\theta_p = 1400\,°C$, (b) at $\theta_p = 1450\,°C$ (the sputtering rates refer to a standard of Ta_2O_5).

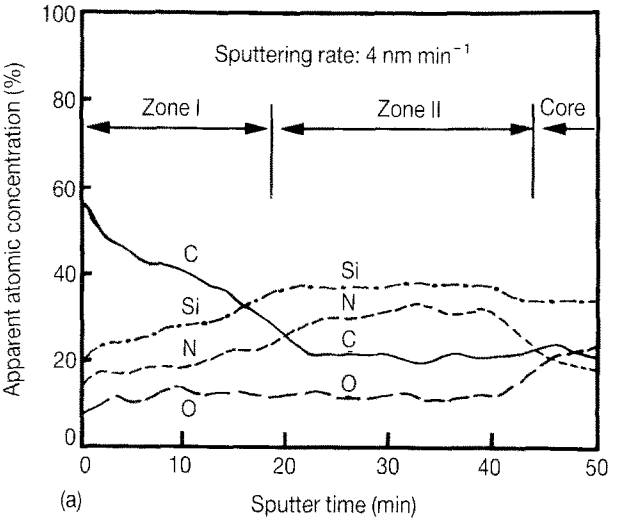

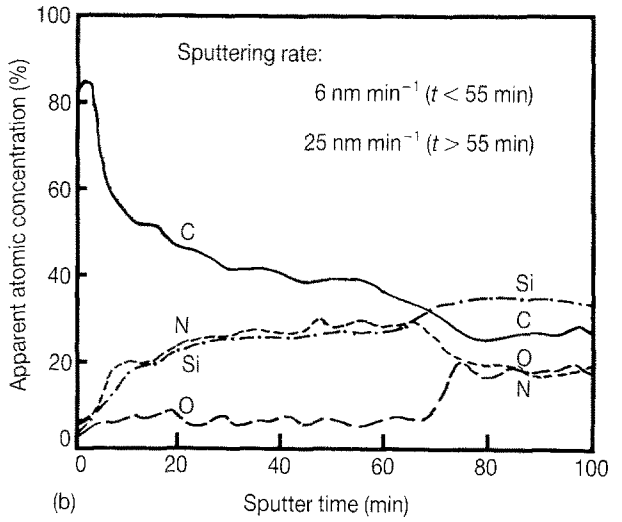

Figure 4 AES depth profile analyses near the filament external surface recorded for Si–C–N–O filaments pyrolysed under a gas flow of nitrogen ($P = 100$ kPa; $Q = 1\,l\,h^{-1}$) during 15 min: (a) at $\theta_p = 1400\,°C$, (b) at $\theta_p = 1450\,°C$ (the sputtering rates are referring to a standard of Ta_2O_5).

order to establish whether or not the chemical composition remained constant through the filament cross-section. The results, given in Figs 3 and 4, were found to depend on both the values of θ_p and the nature of the pyrolysis furnace atmosphere. Generally speaking, for $\theta_p = 1200\,°C$, the chemical composition of the filaments is almost identical in the core and near the external surface, whatever the nature of the pyrolysis atmosphere, but this is no longer true for $\theta_p = 1400\,°C$.

(i) Under argon, a pyrolysis treatment of 15 min at 1400 °C yields a decomposition zone near the external surface of the filament, as shown in Fig. 3a. Starting from the filament surface, a first zone, very rich in carbon, is observed with an apparent thickness of about 30 nm (based on the sputtering rate of a Ta_2O_5 film). It is followed by a second zone (apparent thickness 200 nm) which appears to be enriched in carbon and depleted in silicon and oxygen with respect to the unchanged filament standing just below. When θ_p is slightly raised, i.e. for $\theta_p = 1450\,°C$ and $t = 15$ min, the decomposition process is still more apparent, as shown in Fig. 3b, and thus the decomposition zones are much wider and their respective compositions are much more easily assessed. The first decomposition zone (apparent thickness 150–200 nm) consists of carbon and silicon with a very high percentage of carbon and only trace of oxygen and nitrogen. The second zone, with an apparent thickness of 2.5 μm (i.e. about 25% of the initial filament radius), is both significantly enriched in carbon and depleted in oxygen and nitrogen, with respect to the unchanged filament core. It is of interest to note that the interfaces between the three zones are not sharp (particularly that between zone I and zone II) suggesting that diffusion phenomena might have occurred. Finally, for $\theta_p = 1500\,°C$ and $t = 15$ min, the overall decomposition zone is still more extended (apparent thickness larger than 3 μm).

(ii) Under nitrogen, a pyrolysis treatment of 15 min at 1400 °C results in a significant change in composition near the filament surface, as shown in Fig. 4a. In zone I, i.e. over an apparent thickness of about 60 nm, the filament is progressively enriched in carbon and simultaneously depleted in silicon, nitrogen and oxygen when moving from the inside

towards the surface. Below, i.e. in zone II whose apparent thickness is of the order of 80 nm, the filament is enriched in nitrogen and depleted in both carbon and oxygen with respect to the unchanged core of the filament standing below. It is worthy of note that the elemental concentrations are almost uniform within zone II whereas they exhibit pronounced gradients (particularly that of carbon) across zone I, when θ_p is raised from 1400 °C to 1450 °C, the overall apparent thickness of the two layers (i.e. zone I + zone II) increases up to about 300 nm, the boundary between zone I and zone II being less apparent than for $\theta_p = 1400$ °C (Fig. 4b). On the contrary, for the pyrolysis under an argon atmosphere, the interfaces between the different zones are broad. Finally, for $\theta_p = 1600$ °C, the apparent thickness of the overall modified zone is still larger (i.e. more than 5 μm), the filament surface consisting almost of pure carbon.

3.3. Structure and microstructure

As shown in Fig. 5, the XRD patterns of the Si–C–N–O ex-PCSZ filaments exhibit no sharp diffraction peaks up to $\theta_p = 1400$ °C whatever the nature of the pyrolysis atmosphere, but only a few broad signals of low intensity characteristic of amorphous materials. The filaments pyrolysed under argon undergo a crystallization process, which is very limited for $\theta_p = 1500$ °C, but well apparent at 1600 °C. The main diffraction peaks were assigned to β-SiC and the weak peaks to a mixture of hexagonal α-SiC polytypes. When pyrolysed under nitrogen, the beginning of the crystallization process is noticeable for $\theta_p = 1600$ °C, the XRD pattern showing a very broad feature which might be assigned to the strong 1 1 1 reflection of β-SiC. Thus it appears that the amorphous Si–C–N–O is much more stable when aged under nitrogen, as could be expected.

The fine structure and microstructure of the filaments were studied in a detailed manner by TEM as a function of both θ_p (with $1400 < \theta_p < 1600$ °C) and pyrolysis atmosphere.

(i) Si–C–N–O filaments pyrolysed under argon at $\theta_p = 1400$ °C are heterogeneous in microstructure, as shown in Fig. 6a. A highly porous skin, whose mean thickness is of the order of 200 nm is clearly apparent near the filament surface. However, both the core and the skin of the filament are amorphous on the basis of electron diffraction patterns (Fig. 6b). For $\theta_p = 1450$ °C, the thickness of the skin is significantly enlarged (up to 3 μm) and the boundary between the core and the skin clearly apparent (Fig. 7b). The dark-field images recorded with the aperture in position 2 (see Section 2.2) show that the skin consists mainly of β-SiC tiny crystals (Fig. 7a). Furthermore, a thorough analysis performed in the dark-field imaging mode, the aperture being in position 1, focusing and defocusing the apparatus (a procedure which permits one to ascertain whether given observed faint dots are images of actual objects or artefacts induced by the microscope), showed that free carbon was also present but at a poorly organized state. The mean size of the β-SiC crystals in the skin ranges from 10 nm near the skin–core boundary (Fig. 7a) to 45 nm in the vinicity of the filament surface (Fig. 7b). Finally, the filament core was observed to be still amorphous. For $\theta_p = 1600$ °C, the filament within its whole volume consists mainly of β-SiC crystals whose mean size is of the order of 15–20 nm (some of them being as large as 90 nm) (Fig. 8) Although a thorough analysis for carbon was not performed (according to the procedure described above), it is thought that some free carbon is also present.

(ii) Si–C–N–O ex-PCSZ filaments pyrolysed under nitrogen exhibit a structure and microstructure which have some common features, but also a few differences, with respect to those described in (i). For $\theta_p = 1400$ °C, the filaments are surrounded with a skin, 150 nm thick, whose microtexture is similar to that observed in filaments pyrolysed under argon and their core is amorphous. For $\theta_p = 1450$ °C, the skin has now a thickness of 500 nm, both the skin and the core being amorphous, as shown in Fig. 9. Finally, for $\theta_p = 1600$ °C, the amorphous material resulting from the organic/inorganic transition of PCSZ has been

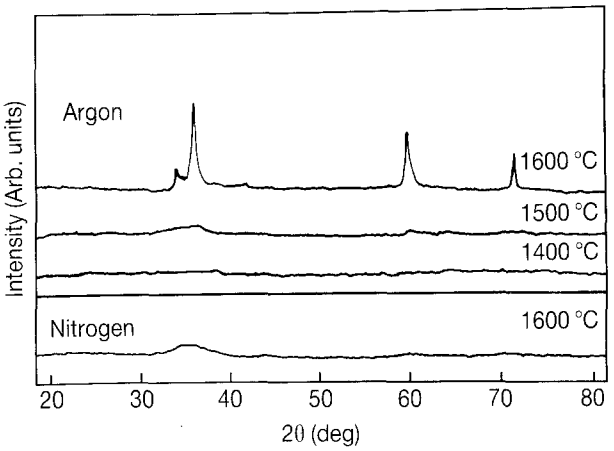

Figure 5 XRD-patterns of ex-PCSZ Si–C–N–O filaments pyrolysed at increasing temperatures under an argon or nitrogen atmosphere.

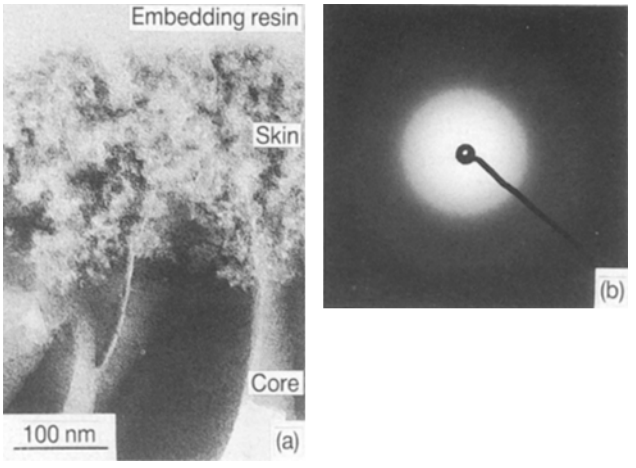

Figure 6 TEM analysis of a Si–C–N–O ex-PCSZ filament pyrolysed at 1400 °C under an argon atmosphere: (a) bright-field picture showing the occurrence of a skin with a thickness of about 200 nm; (b) diffraction pattern of either the skin or the core, characteristic of an amorphous material.

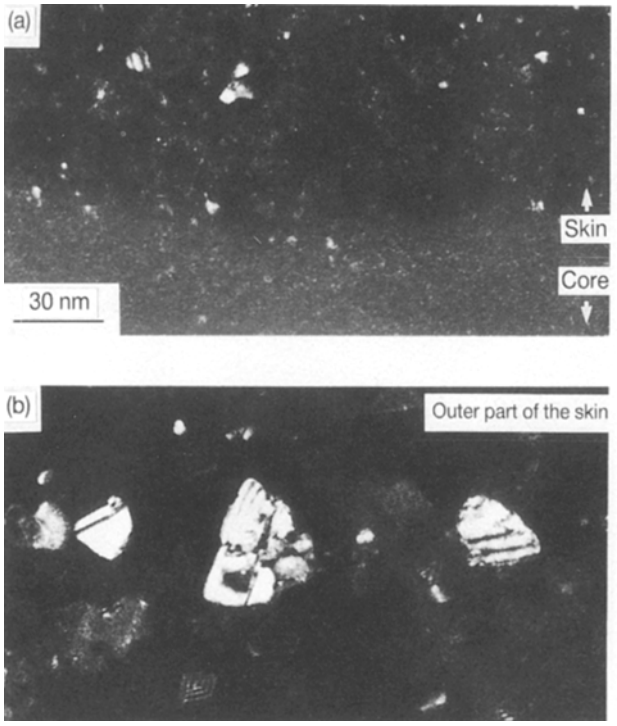

Figure 7 Dark-field TEM images (aperture in position 2) of a Si–C–N–O ex-PCSZ filament pyrolysed at 1450 °C under argon atmosphere from the skin: (a) near the skin/core boundary, (b) near the filament surface.

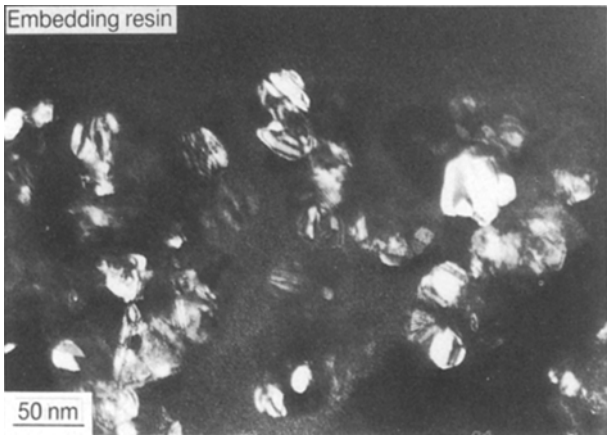

Figure 8 Dark-field images (aperture located in position 2) of a Si–C–N–O ex-PCSZ filament pyrolysed at 1600 °C under argon atmosphere, showing large size β-SiC crystals.

totally converted into β-SiC crystals having size ranges from 1.2–4 nm whereas whiskers of either α- or β-Si_3N_4 are present at the filament surface.

3.4. Morphology and density

Si–C–N–O ex-PCSZ filaments exhibit a cylindrical geometry. The variations of both the filament diameter and density, as a function of θ_p, are shown in Fig. 10. During the organic/inorganic transition, i.e. for $550 < \theta_p < 850$ °C, an important shrinkage occurs, due to the evolution of gaseous species (mainly CH_4 or H_2), and simultaneously the density increases from 1.2 g cm^{-3} to 2.2 g cm^{-3}. Then, within $850 < \theta_p < 1400$ °C corresponding to the plateau of the TGA

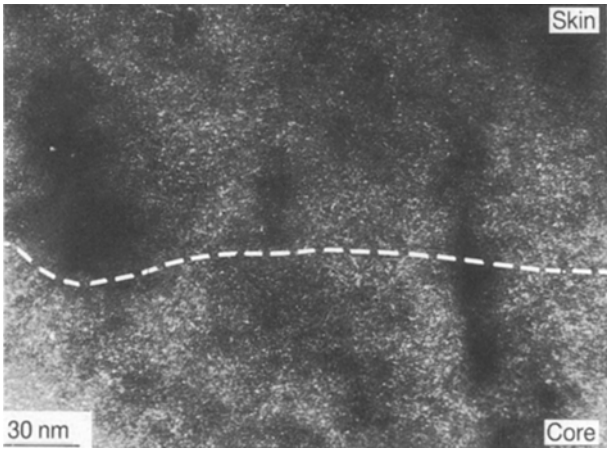

Figure 9 Dark-field images (aperture located in position 2) of a Si–C–N–O ex-PCSZ filament pyrolysed at 1450 °C (15 min) under a nitrogen atmosphere, from an area located near the skin/core boundary showing that it does not contain any crystals of β-SiC of significant size.

curve (see Fig. 1), the variations of diameter and density with θ_p are much less pronounced (the value of density at 1200 °C being of the order of 2.5 g cm^{-3}). Finally, beyond 1400 °C, the phenomena which are observed depend on the nature of the pyrolysis atmosphere, as already mentioned: (i) when the pyrolysis is performed in argon, a dramatic decrease in diameter occurs which is undoubtedly related to the decomposition process of the filament yielding an evolution of CO and N_2 (Figs 1 and 2), whereas (ii) when it is performed under nitrogen, the diameter decrease is less pronounced.

For $850 < \theta_p < 1200$ °C, the failure surface of the filaments, as observed by scanning electron microscopy (SEM), is typical of an amorphous material whatever the nature of the pyrolysis atmosphere. In contrast for $\theta_p > 1200$ °C, the features of the failure surface depends on the nature of the flowing in the pyrolysis furnace.

(i) When pyrolysed under argon, e.g. at 1450 °C, the filaments consist clearly of two concentric parts: a porous skin, mechanically poorly resistant, with a rough failure surface, weakly bonded to a much stronger core (as evinced from delamination taking place at the skin–core boundary and peeling phenomena) (Fig. 11a). It is noteworthy that a similar behaviour was previously reported by Okamura *et al.*, for the related ex-PCS Si–C–O filaments pyrolysed under the same conditions [33]. These features are consistent with the results of the AES and TEM analyses and suggest that the skin corresponds to that part of the filament where the decomposition/crystallization process took place during the pyrolysis treatment, whereas the core is the untransformed part of the filament. When θ_p is raised from 1450 °C to 1500 °C, the decomposition/crystallization process proceeds to completion with the result that the failure surface is now homogeneously rough (Fig. 11b) which means that the skin observed for lower θ_p values has continued to grow at the expense of the amorphous core and finally reached the centre of the filament.

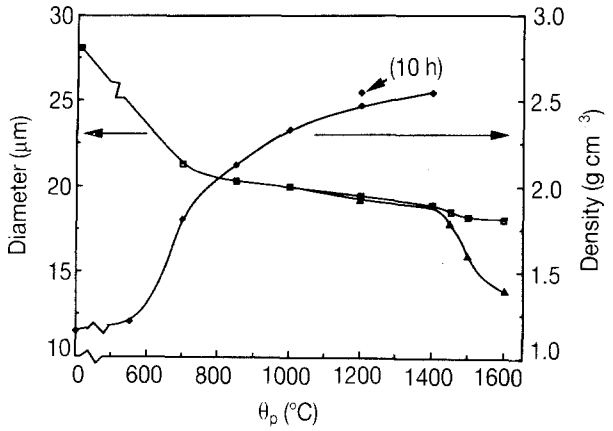

Figure 10 Variations of the diameter under N_2 (■) and under Ar (▲) density (Ar) of ex-PCSZ Si–C–N–O filaments as a function of the pyrolysis conditions (temperature and atmosphere).

In addition, a very thin layer of a material weakly bonded to the filament is present at the filament surface.

(ii) When pyrolysed under nitrogen at 1450 °C, the filaments no longer exhibit a dual failure surface (Fig. 12a). Conversely, for $\theta_p = 1600$ °C, crystallization of the amorphous Si–C–N–O material, as well as some interaction with the gas phase, have obviously taken place (Fig. 12b) as evinced from the rough failure surface and occurrence of crystals on the filament surface. In addition, large bulk crystals and whiskers are present on the filament surface as previously reported by Lewis in his study of the ageing of Si–C–Ti fibres under nitrogen [34].

3.5. Electrical conductivity

The thermal variations of the electrical conductivity of ex-PCSZ Si–C–N–O filaments pyrolysed at various temperatures under an argon atmosphere, are shown in Fig. 13a. Generally speaking, the filaments exhibit a semi-conducting behaviour, the variations as a function of θ_p, of both the electrical conductivity measured at 500 K, σ_{500}, and the apparent activation energy, E_a, calculated from the slope of the $\log_{10}\sigma = f(1/T)$ graphs, shown in Fig. 13b. The electrical conductivity remains low for the filaments which have been pyrolysed at low θ_p values. However, a change in the conductivity mechanism is observed to occur at $\theta_p = 1400$ °C which might be related to a transition from a semi-conductor behaviour to a semi-metallic behaviour, as we have previously reported for ex-PCS bulk or filamentary ceramics [7, 35] and for ex-PCSZ bulk ceramic samples [28].

3.6. Mechanical properties at room temperature

The variations of both the tensile failure stress, σ^R, and Young's modulus, E, measured at room temperature, as a function of θ_p, are shown in Fig. 14a and b for filaments pyrolysed either under argon or nitrogen atmosphere. The failure stress, σ^R, increases rapidly as θ_p is raised during the organic/inorganic transition

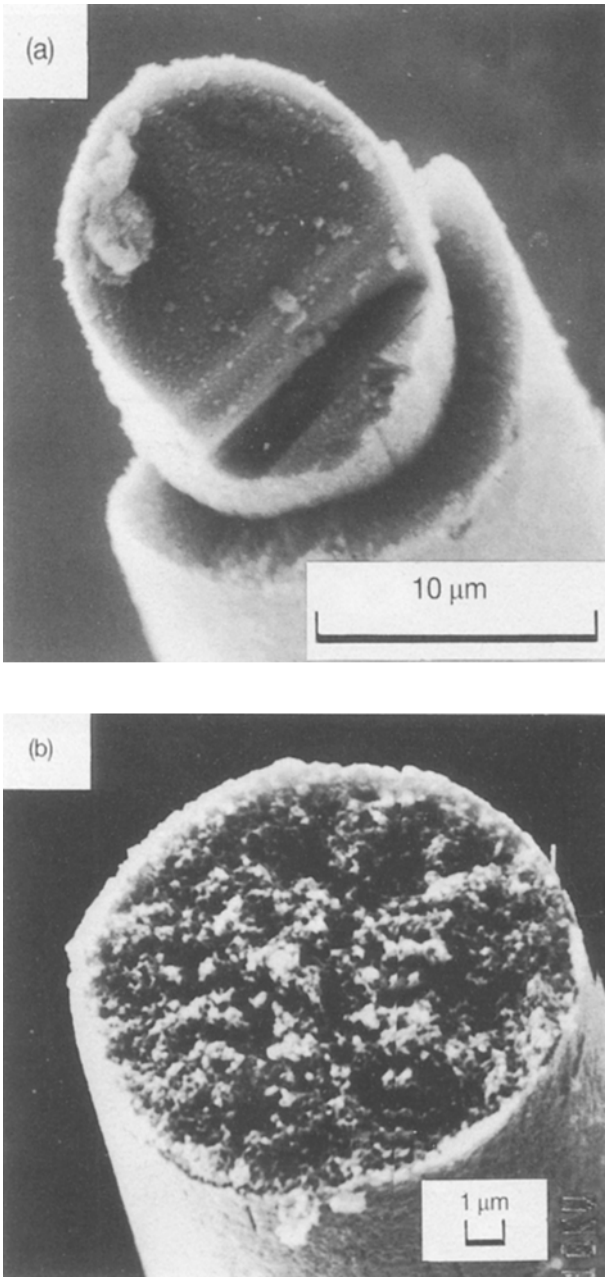

Figure 11 Failure surfaces of ex-PCSZ Si–C–N–O filaments pyrolysed under an argon atmosphere at various temperatures: (a) $\theta_p = 1450$ °C; (b) $\theta_p = 1500$ °C (in all cases, the filaments were tensile loaded at room temperature).

(i.e. for $500 < \theta_p < 850$ °C). Then, it increases only very slowly to reach a maximum value at about $\theta_p = 1200$ °C, which is slightly dependent on the nature of the pyrolysis atmosphere (i.e. it is slightly higher for the filaments which have been pyrolysed in nitrogen). Beyond this value, σ^R decreases rather rapidly as θ_p is still raised. However, the residual failure stress for $\theta_p = 1400$ °C is still equal to 70%–75% of the maximum, a result to be compared with the much lower value (i.e. 40%) reported by Bouillon *et al.* for the related ex-PCS Si–C–O filaments prepared and tested under similar conditions [8]. Futhermore, the ex-PCSZ Si–C–N–O filaments pyrolysed at 1600 °C under nitrogen, although weak, can still be handled, which is not the case when the pyrolysis has been performed under argon.

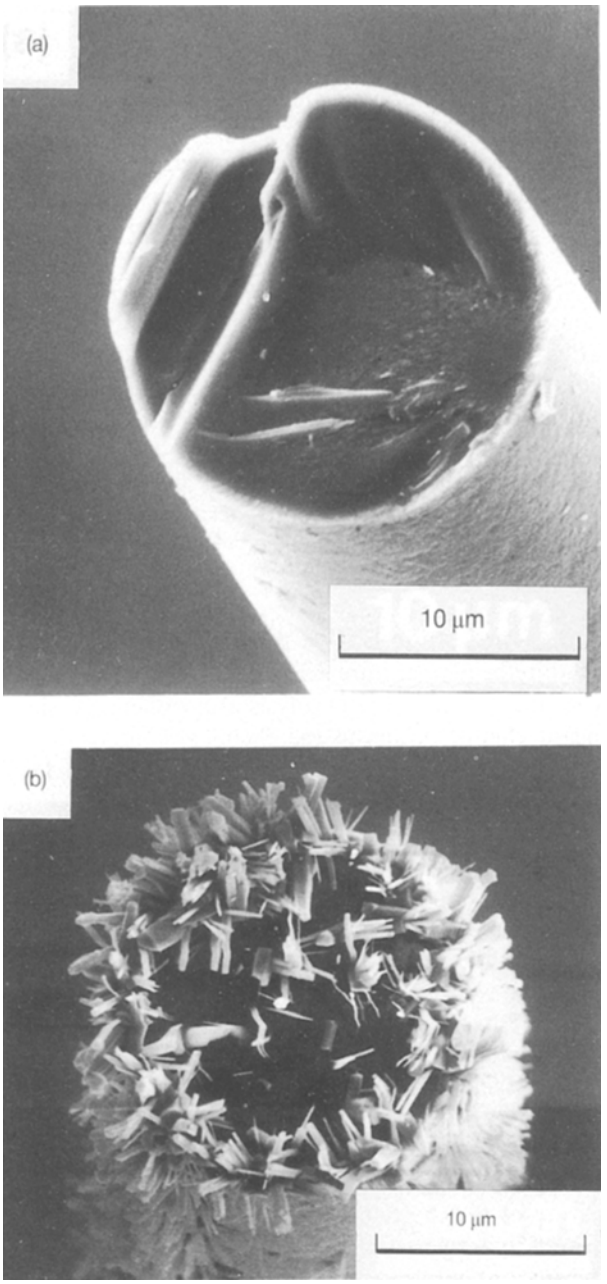

Figure 12 Failure surfaces of ex-PCSZ Si–C–N–O filaments pyrolysed under a nitrogen atmosphere at various temperatures: (a) $\theta_p = 1450\,°C$; (b) $\theta_p = 1600\,°C$ (in all cases, the filaments were tensile loaded at room temperature).

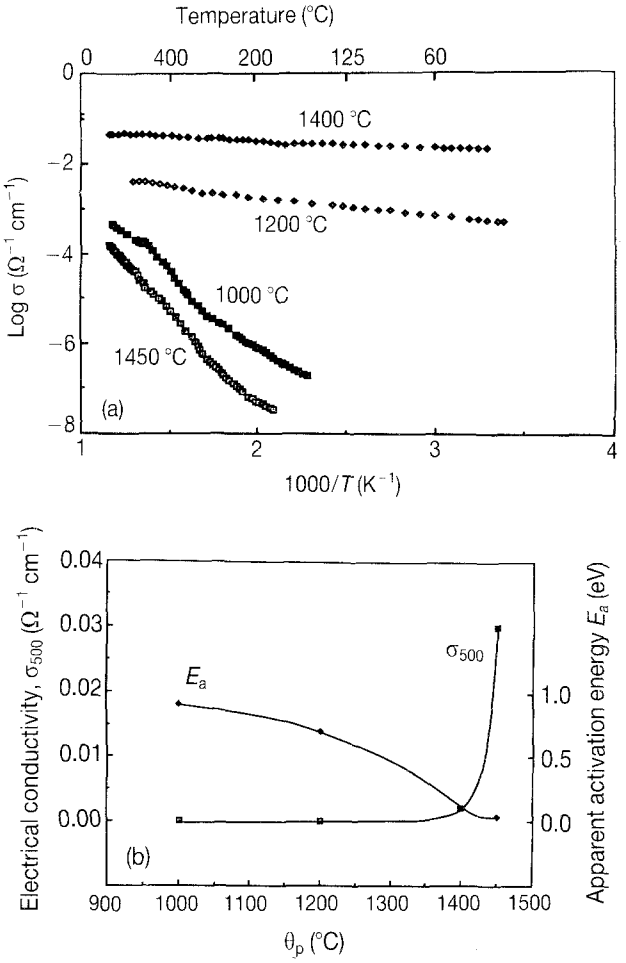

Figure 13 Electrical behaviour of ex-PCSZ Si–C–N–O filaments pyrolysed at various temperatures under argon atmosphere: (a) thermal variations of the electrical conductivity measured at 500 K as a function of the pyrolysis temperature θ_p; (b) variation of σ_{500} and E_a with θ_p.

The Young's modulus of Si–C–N–O filaments increases continuously as θ_p is raised from 700 °C to 1400–1450 °C and it decreases dramatically beyond this upper limit. The benefit of the pyrolysis under nitrogen, mentioned above for the failure stress, is almost effective for the stiffness (Fig. 14b).

4. Discussion

On the basis of the data reported in Section 3, the pyrolysis of melt-spun/oxygen-cured PCSZ filaments under argon or nitrogen atmosphere can be discussed by considering four successive temperature domains (see Fig. 1): (i) $25 < \theta_p < 500\,°C$ (outgasing of the cured-polymer), (ii) $500 < \theta_p < 850\,°C$ (organic/inorganic transition), (iii) $850 < \theta_p < 1400\,°C$ (densification), and (iv) $1400 < \theta_p < 1600\,°C$ (decomposition/crystallization process when pyrolysis is performed under argon or a nitriding/crystallization process when it is performed in nitrogen).

4.1. First stage $25 < \theta_p < 500\,°C$

As shown in Fig. 1, oxygen-cured PCSZ filaments undergo a small weight loss when θ_p is raised from room temperature to 500 °C. This weight loss (which is of the order of 2 wt %), might be due to an evolution of water vapour and some oligomers. Water is thought to be related to the oxygen-curing process, known to release H_2O if one assumes that it takes place with the formation of Si–O–Si bridges as proposed by Hasegawa and Okamura [36].

The evolution of oligomers has been already mentioned by Poupeau *et al.* [37] or Hasegawa and Okamura [36], for oxygen-cured PCS-polymers. It has been also reported to occur during the first stage of the pyrolysis of uncured-PCS by Bouillon *et al.* [7] or uncured-PCSZ by Mocaer *et al.* [28], when it was responsible for very large weight losses (e.g. about 22 wt % for the uncured PCSZ-II used in the present study).

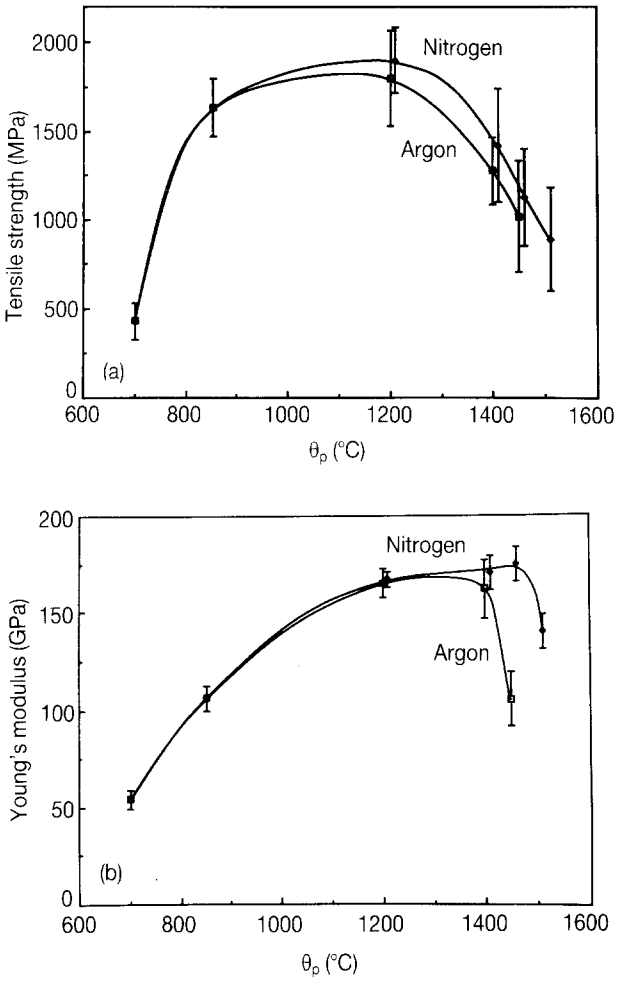

Figure 14 Variations of the mechanical characteristics of ex-PCSZ Si–C–N–O filaments measured in tensile at room temperature, as a function of the pyrolysis conditions, i.e. θ_p and nature of the atmosphere: (a) ultimate failure stress, σ^R; (b) Youngs' modulus, E.

4.2. Second stage $500 < \theta_p < 850\,^\circ C$

The organic/inorganic conversion of the oxygen-cured PCSZ filaments occurs within the temperature range 500–850 °C with the first significant weight loss (about 10 wt %) observed during the pyrolysis (Fig. 1). This weight loss can be assigned mainly to an evolution of methane and hydrogen (resulting from broken organic bonds: pendent groups), on the basis of the detailed study previously published by us [28, 35].

The organic/inorganic transition results in amorphous filaments whose chemical composition corresponds to the overall formula $SiC_{0.8}N_{0.38}O_{0.58}(H)$. The quantitative analysis of hydrogen e.g. by gas phase analysis or nuclear magnetic resonance (NMR), which requires large samples, was not carried out in the present work as already mentioned. However, it is anticipated that hydrogen is present in rather significant amounts in the amorphous filaments for $\theta_p = 850\,^\circ C$, on the basis of the data on the pyrolysis of the uncured PCSZ [28] previously published. As an example, the amorphous residue resulting from the pyrolysis of the material referred to as PCSZ-I (whose degree of cross-linking is much lower than that of PCSZ-II used in the present study), was given to correspond to the overall $SiC_{0.86}N_{0.50}O_{0.03}H_{0.8}$ for $\theta_p = 850\,^\circ C$, i.e. the hydrogen concentration (established by gas phase analysis) was of the order of 1.7 wt %. Although hydrogen is present at a low concentration, it is thought to play an important role in the stabilization of the amorphous state of the pyrolytic residue.

This transition results in an important shrinkage of the filament, as could be expected. Thus, the filament diameter decreases from 28 μm to 20 μm (i.e. by 28%) and simultaneously the density increases from 1.15 $g\,cm^{-3}$ to 2.20 $g\,cm^{-3}$ (i.e. by about 90%) when the temperature is raised from 500 °C to 850 °C (Fig. 10). These features are consistent with the weight loss of 10% above reported. Finally, the organic/inorganic transition dramatically increases the failure tensile stress of the filament and, to a less extent, its stiffness, as shown in Fig. 14, a feature which is common observation for fibres deriving from oxygen-cured organosilicon fibres.

4.3. Third stage $850 < \theta_p < 1400\,^\circ C$

Within the temperature range 850–1400 °C, and whatever the nature of the pyrolysis atmosphere, no significant change occurs in the chemical composition of the amorphous filament, as evinced from the plateau observed in the TGA curve (Fig. 1) and the data listed in Table I. The main phenomenon taking place is thought to be a continuous evolution of hydrogen (Fig. 2b). Hydrogen might result mostly from (i) the splitting of residual methyl groups still present in the amorphous pyrolytic residue (incomplete mineralisation), as well as (ii) the formation of carbon BSUs (isolated basic structural units are turbostratic stacks of two to three aromatic layers of about ten aromatic carbon cycles [38]). To a less extent, hydrogen could also result from the cleavage of residual Si–H bonds that would not have been involved in the oxygen-curing process or thermal cross-linking. Whatever the nature of the mechanisms responsible for the evolution of hydrogen, it clearly appears from Fig. 2b that the amount of released hydrogen is qualitatively much lower for the oxygen-cured PCSZ-II filaments than for the uncured ones. This feature suggests that the hydrogen concentration in the oxygen-cured filaments obtained at $\theta_p = 850\,^\circ C$ is much lower than the value, i.e. 1.7 wt %, mentioned above for the uncured PCSZ-I bulk samples.

The hydrogen evolution yields a new but very small weight loss (< 1 wt %). More interestingly, it also results in a significant densification, as evinced by the increase in density (from 2.10 $g\,cm^{-3}$ to 2.50 $g\,cm^{-3}$ when θ_p is raised from 850 °C to 1400 °C). This result obviously suggests that some significant change occurs in the structure of the amorphous pyrolytic residue which has to be related to the cleavage of bonds involving hydrogen. The densification process and structural change result in a significant increase in the stiffness of the filament (E increases from 105 GPa to 165 GPa, i.e. by about 60% when θ_p is raised from 850 °C to 1200 °C). Otherwise, the tensile failure stress remains almost unchanged (σ^R = 1650 and 1880 MPa for θ_p = 850 and 1200 °C, respectively), the filaments exhibiting a failure surface typical of an amorphous

material within this temperature range. These features are very different from those reported for the oxygen-cured ex-PCS filaments whose tensile failure stress undergoes a sharp maximum for θ_p close to 1200 °C [4]. This difference could be explained by the fact that the ex-PCSZ filaments remain amorphous up to about 1400 °C, whereas the ex-PCS filaments undergo a decomposition/crystallization process for θ_p = 1200 °C (or even slightly below).

The higher stability of the amorphous state in the ex-PCSZ Si–C–N–O filaments seems to be due to the higher amount of heteroatoms (i.e. both nitrogen and oxygen) present in the tetrahedral coordination of silicon which prevents the growth of SiC crystals. On the basis of our NMR study [28] on the uncured PCSZ polymers, the evolution of the tetrahedral coordination around silicon during the pyrolysis of oxygen-cured ex-PCSZ filaments could be explained as follows.

(i) In the starting uncured PCSZ-II, the following main tetravalent surrounding are present for silicon

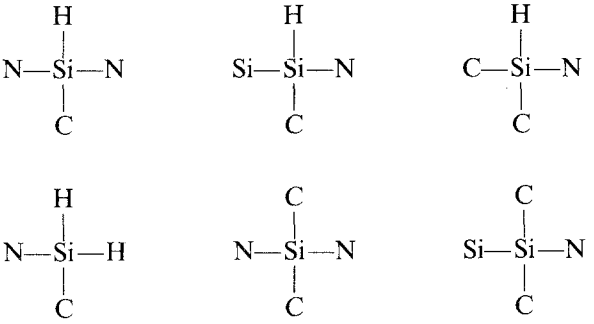

(ii) Assuming that the oxygen-curing process involved mainly oxidation of the Si–H bonds according to a mechanism previously reported by Hasegawa [36] and only to a negligible extent oxidation of Si–C or remaining Si–Si bonds [27], the coordination around silicon could be the following after the curing step

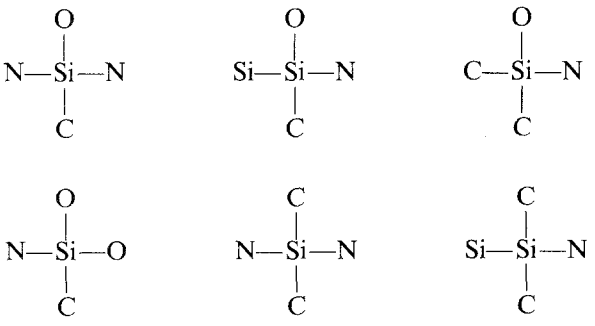

(not including the remaining SiH bonds).

(iii) When θ_p is raised, i.e. during the organic/inorganic transition and above, atomic rearrangements involving methyl groups insertion into Si–Si bonds and dehydrogenation which might occur according to mechanisms analogous to those described by Taki *et al.* [39] are thought to take place, resulting in the following silicon sites for high θ_p values

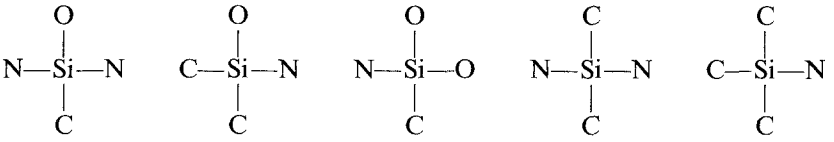

$(SiCN_2O)$ (SiC_2NO) $(SiCNO)$ (SiC_2N_2) (SiC_3N)

The silicon sites actually present in the amorphous Si–C–N–O material resulting from the organic/inorganic conversion in oxygen-cured ex-PCSZ filaments should not be very different from those mentioned by Lipowitz *et al.* in their study of fibres spun from nitrogen-containing precursors and cured with water vapour [22].

It clearly appears from the above discussion that the occurrence of the heteroatoms (nitrogen and oxygen) responsible for the formation of the binary (i.e. SiC_2N_2 and SiC_3N) and ternary (i.e. SiC_2NO, $SiCN_2O$ and $SiCNO_2$) tetrahedral silicon sites prevents that of the SiC_4 sites which would lead to the growth of silicon carbide at high temperature [9]. Moreover, the fact that (i) there are two different heteroatoms in ex-PCSZ oxygen-cured filaments instead of only one in ex-PCS oxygen-cured filaments, and (ii) the overall heteroatoms concentration is higher (i.e. 36 at % at 1200 °C, present work) in the former than in the latter (i.e. ≈20 at %, according to [8]), might explain the higher thermal stability of the amorphous state observed for ex-PCSZ Si–C–N–O filaments.

Finally, the electrical conductivity of the amorphous ex-PCSZ filaments remains low up to θ_p = 1400 °C (Fig. 13), i.e. as long as the filaments consist of a homogeneous single amorphous silicon oxycarbonitride. The electrical behaviour appears to be that of a semi-conducting material with an apparent activation energy of the order of 0.7–0.9 eV, close to that of polycrystalline SiC: $E_a \approx 0.6$ eV.

4.4. Fourth stage $1400 < \theta_p < 1600$ °C

The data reported in Section 3 show that a strong change occurs in the filaments when $\theta_p > 1400$ °C. Moreover, because the result depends on the nature of the pyrolysis atmosphere, the discussion will be divided into two parts.

4.4.1. Pyrolysis under an argon atmosphere

A decomposition process takes place in ex-PCSZ oxygen-cured filaments when θ_p = 1400 °C as pointed out from the AES and TEM data (Figs 3a, 6). It starts from the filament surface yielding an amorphous skin (0.2 μm thick for t = 15 min) enriched in carbon and

depleted in both silicon and oxygen whereas the core remains unchanged in composition and microstructure. On the basis of the results of the gas-phase analysis (Fig. 2a), EPMA analysis (Table I) and AES analysis (Fig. 3a), it seems that the decomposition process at this somewhat low temperature involves mainly Si–O bonds. It results in evolution of oxygen-containing species (i.e. CO and probably SiO but the latter could not be detected by mass spectroscopy owing to the nature of the experimental apparatus). The alteration of the filament surface yields a significant decrease, about 30%, of the tensile failure stress at room temperature, which is thought to be related to the occurrence of new surface flaws, whereas the Young's modulus still remains unchanged. However, this drop in failure strength although significant is much lower than that, i.e. $\approx 60\%$, previously reported for ex-PCS filaments treated under similar conditions [8]. Finally, as shown in Fig. 13, the electrical conductivity at 500 K slightly increases when θ_p is raised from 1200 °C to 1400 °C, owing to the contribution of the carbon-rich skin assumed to have a high electrical conductivity, but whose thickness is still very small. Conversely, the change in the apparent activation energy is already significant ($E_a = 0.7$ and 0.1 eV when $\theta_p = 1200$ and 1400 °C, respectively) suggesting that a new conduction mechanism, involving free carbon, is taking place.

For $\theta_p = 1450$ °C and $t = 15$ min, the skin is thicker and exhibits a dual structure, as shown from the AES depth profiles (Fig. 3b); its outer part is strongly enriched in carbon, whereas its inner part is a mixture of β-SiC tiny crystals and free carbon almost free of both oxygen and nitrogen. The skin is only weakly bonded to the core (which remains amorphous and unchanged in composition) as evinced from delamination at the skin/core boundary (Fig. 11a, b). All these results suggest that a complex decomposition/crystallization process of the amorphous silicon-oxycarbonitride is taking place, its front moving radially versus time from the external surface towards the filament centre. The decomposition process involves now both the Si–O and Si–N bonds, as shown by the simultaneous evolution of CO and nitrogen (Fig. 2a) which is responsible for the important weight loss observed for $1400 < \theta_p < 1600$ °C (Fig. 1). A similar dual CO/N_2 evolution has been also mentioned by Jaffe *et al.* [40] in their study of the pyrolysis of Si–C–N–O fibres prepared from methylpolydisilazane (MPDZ). The decomposition of the amorphous Si–C–N–O material yields a mixture of β-SiC crystals and free carbon in which the size of the former increases when moving radially from the inner part of the skin towards the filament surface (Fig. 7). These features could be explained by the fact that the loss of the heteroatoms (nitrogen, oxygen) allows the formation of SiC_4 sites and therefore the growth of the SiC phase. Moreover, because the SiC crystals in the outer part of the skin have been formed first, they could grow further (as the front is moving inwards) to a size larger than that of the crystals being formed at the skin/core boundary. Furthermore, the decomposition products mixture (i.e. β-SiC + C) appears to be itself unstable under the experimental conditions, because the outer part of the skin is observed to be depleted in silicon (Fig. 3b) and consists almost uniquely of pure carbon in the very vicinity of the filament surface. This feature means that gaseous silicon-based species (which could be either SiO or silicon itself) are formed and escape from the skin, as previously suggested by Johnson *et al.* [41] or by us [8] for ex-PCS oxygen-cured materials. This decomposition/crystallization process explains all the changes in the filament characteristics reported in Section 3. Thus, the shrinkage of the filament diameter (Fig. 10) results directly from the fact that the formation of the skin involves an important loss of matter. The lowering of both σ^R and E (Fig. 14) could be assigned to a reduction of the actual load-bearing cross-section if one assumes that load is mainly carried by the filament core (which still remains unchanged for this θ_p value) thus neglecting the contribution of the weak skin. Similarly, the electrical conductivity at 500 K increases by a factor of 15 when θ_p is raised from 1400 °C to 1450 °C: it is noteworthy that the skin cross-section increases exactly in the same proportion. This result suggests that the electrical conductivity of the filament is mainly controlled by that of the highly conducting β-SiC + C mixture, for $\theta_p > 1400$ °C.

For $\theta_P = 1500$ °C, the fraction of the filament cross-section which has undergone the decomposition/crystallization process is now very large, as shown from the weight loss value, i.e. 33%, and the diameter shrinkage (about 20%). The filament, whose overall composition corresponds to the formula $SiC_{1.17}N_{0.15}O_{0.1}$, is a mixture of β-SiC + C with some residual Si–C–N–O matrix. It is so weak mechanically that it could not be quantitatively tensile tested (its failure surface being almost entirely rough).

Finally, for $\theta_P = 1600$ °C and $t = 15$ min, the decomposition/crystallization process has proceeded to completion with an overall weight loss of 56% and the diameter shrinkage of 30% (the final diameter being of the order of 14 μm). As shown in Table I, almost all the heteroatoms (nitrogen, oxygen) escape from the filament (the residual concentration in oxygen and nitrogen being each of the order of 0.5 at %) and the pyrolytic residue is a carbon-rich β-SiC + C mixture (the C/Si atomic ratio being 1.30) in which the size of the β-SiC crystals is 15–20 nm.

To summarize, the variations of the chemical composition of the filament within the temperature range 850–1600 °C, i.e. from the end of the organic/inorganic transition to that of the decomposition/crystallization of the Si–C–N–O amorphous material, can be depicted on the basis of the EPMA and TGA analyses (neglecting hydrogen) by the following overall equation

$$35\,Si\,C_{0.83}N_{0.4}O_{0.57} \rightarrow 19\,SiC + 6\,C + 16\,SiO\uparrow + 4\,CO\uparrow + 7\,N_2\uparrow \quad (1)$$

in which the molar ratio of the gaseous species SiO and CO is of the order of 4, i.e. close to that, 5, reported by Johnson *et al.* [41] in their study of ex-PCS fibres (Nicalon, Nippon Carbon) heated at ≈ 1400 °C in a Knudsen effusion cell.

4.4.2. Pyrolysis under a nitrogen atmosphere

When the pyrolysis is performed under a nitrogen atmosphere, the decomposition of the amorphous Si–C–N–O material starts also at about 1400 °C. The skin, which is amorphous and has an overall thickness of about 0.15 μm, consists of two adjacent sub-layers (Fig. 4a): (i) the inner sub-layer is depleted in both carbon and oxygen whereas it is enriched in nitrogen, with respect to the core, and (ii) the outer sub-layer exhibits a carbon concentration which progressively increases when moving towards the filament surface. The chemical composition of the core is homogeneous and similar to that observed at lower temperatures, i.e. the decomposition process has been limited to the skin. As discussed in Section 4.1.1, the growth of the skin significantly lowers the tensile failure stress at room temperature, but conversely, it has almost no effect on the Young's modulus.

For $\theta_P = 1450$ °C, the overall thickness of the skin is about 0.5 μm. With respect to that described in Section 4.1 (argon atmosphere), it exhibits two important differences: (i) its concentration in nitrogen is much higher (it is even higher than that of the unchanged core) and simultaneously that in carbon is comparatively lower (although it is close to 100% in the very vicinity of the surface in both cases), and (ii) the skin remains amorphous (whereas it was already crystallized for the argon atmosphere pyrolysis). These features suggest the occurrence of two radial diffusion fluxes across the skin: a flux of oxygen-based species (i.e. CO and SiO) from the skin/core boundary towards the filament surface and a flux of nitrogen in the opposite direction. The tensile failure stress still decreases when θ_P is raised from 1400 °C to 1450 °C suggesting that the failure of the filament is controlled by the flaw population of the skin and thus that the bonding between the skin and the core is strong, in agreement with: (i) the absence of delamination at the skin/core interface, and (ii) the conclusions previously drawn by Fukunaga and Goda for ex-PCS fibres [42]. Conversely, the Young's modulus at room temperature remains almost unchanged (whereas it has already undergone a significant drop for the filament heated at the same temperature but under argon atmosphere) (Fig. 14).

For $\theta_P = 1500$ °C, the fraction of the filament which has seen the decomposition process is still higher and the majority of the filament consists of a still amorphous material whose overall composition is enriched in nitrogen and depleted in oxygen. The tensile failure strength is low but still measurable (i.e. $\sigma^R = 1000$ MPa) whereas this is no longer the case for the filaments pyrolysed under an argon atmosphere, as mentioned in Section 4.1.1. Simultaneously, the stiffness of the filament begins to decrease ($E \approx 185$ and 140 GPa for $\theta_P = 1450$ and 1500 °C, respectively).

Finally, for $\theta_P = 1600$ °C and $t = 15$ min., the conversion process has now proceeded to completion and the filament is enriched in nitrogen and depleted in oxygen over its entire cross-section. Its overall composition is homogeneous and corresponds to the formula $SiC_{0.8}N_{0.7}O_{0.2}$. The overall pyrolysis process results in a weight loss which means that the evolution of the oxygen-based species (thought to be CO and SiO) has been only partly balanced by the absorption of nitrogen. However, the overall diameter shrinkage is much more limited (i.e. 10%) than for the pyrolysis under argon (i.e. 30%) (Fig. 10). From a structural point of view, it is thought that the filament remains mostly amorphous even for $\theta_p = 1600$ °C (Fig. 5), the heteroatoms (i.e. nitrogen present in large amount (26 at %) and, to a less extent, oxygen whose atomic concentration is still equal to 7%, as shown in Table I) preventing the formation of the SiC_4 sites and thus the growth of the SiC phase. However, and as shown from the TEM data, β-SiC crystals are being formed at this temperature but their mean size (i.e. 1–2 nm) is much lower than that (i.e. 15–20 nm) observed in the filaments which have been treated under argon at the same temperature. Thus, the impeding effect of nitrogen upon the formation of crystalline β-SiC at a temperature as high as 1600 °C is clearly established. Finally, the Si_3N_4 whiskers formed on the filament surface (Fig. 12b) could result from a reaction involving SiO and nitrogen, according to the following equation

$$3SiO + 2N_2 \rightarrow Si_3N_4 + 3/2O_2 \qquad (2)$$

To summarize, it seems clearly established that the main phenomenon which takes place at high temperatures ($\theta_P > 1400$ °C) during the pyrolysis of ex-PCSZ oxygen-cured filaments under nitrogen atmosphere, is a decomposition/nitriding process which releases most of the oxygen picked up during the curing step, increases the nitrogen concentration and impedes the growth of β-SiC cystals. Although the mechanical properties are improved with respect to those of the filaments treated under argon, the variations of the tensile failure strength at room temperature as a function of θ_p are very similar but conversely the value of θ_p at which the Young's modulus falls is shifted by about 100 °C towards the high-temperature side.

5. Conclusion

Two important phenomena occur during the pyrolysis of model monofilaments prepared by PCSZ melt-spinning and oxygen-curing.

(i) The organic/inorganic transition, which takes place within the temperature range 500–850 °C with a first important weight loss and diameter shrinkage related to an evolution of CH_4 and H_2, yields an amorphous silicon-oxycarbonitride filament still containing hydrogen. This amorphous material undergoes only minor changes, i.e. a densification process, which might be related to an evolution of hydrogen, within a wide temperature range (from 850 to about 1400 °C).

(ii) A decomposition/crystallization or decomposition/nitriding process, depending on whether the pyrolysis is performed under argon or nitrogen, respectively, takes place beyond about 1400 °C. Under argon, the decomposition of the amorphous material yields an evolution of gaseous oxides (SiO and CO) and nitrogen responsible for a second weight loss and

diameter shrinkage, on the one hand, and a pyrolytic residue consisting of a mixture of β-SiC and carbon which is almost free of any heteroatoms (nitrogen, oxygen) and whose state of crystallization increases as temperature is raised, on the other hand. Under nitrogen, there is both a decomposition of the amorphous material (involving the Si–O bonds) with an evolution of gaseous oxides (presumably SiO and CO) and an absorption of nitrogen, yielding a much limited weight loss and diameter shrinkage, on the one hand, and a pyrolytic Si–C–N (O) residue which remains partly amorphous up to 1600 °C, the growth of β-SiC crystals of large size being impeded by the heteroatoms (mainly nitrogen) on the other hand.

The tensile failure stress at room temperature increases sharply during the organic/inorganic transition and its value undergoes a maximum for a pyrolysis temperature of about 1200 °C, then it decreases owing to the unstability of the amorphous Si–C–N–O filament. The increase of the stiffness at room temperature, according to the pyrolysis temperature is more regular, the highest value being achieved for 1400–1500 °C. The effect of the pyrolysis atmosphere on the mechanical properties is not very important below 1200 °C and significant above (the best results being obtained under nitrogen).

Finally, the Si–C–N–O filaments exhibit a semiconducting behaviour when pyrolysed under argon beyond about 1400 °C and a semi-metallic behaviour (thought to be related to the occurrence of carbon), over this temperature.

Because the oxygen heteroatoms introduced in the material during the curing step are mainly responsible for the decomposition process taking place at high temperatures ($\theta_p > 1200$ °C) and the correlated dramatic drop in the mechanical properties, it is anticipated that better materials could be obtained by changing the curing process in order to avoid the introduction of oxygen. This matter will be the subject of a forthcoming article.

Acknowledgements

This research was done within the framework of a national programme of research on organosilicon precursors involving CNRS, the French Ministry of Defense (DRET), Rhône–Poulenc (RP) and Société Européenne de Propulsion (SEP) whose support is acknowledged. The authors are more particularly indebted to M. Lahaye (Cumemse-UB1), P. Dordor, E. Marquestaux (LCS-CNRS), G. Bourgeois (CES-AMO-UB1), and E. Chassagneux (RP) for their contribution to the EPMA/AES, electrical conductivity and gas-phase analyses, respectively, as well as to P. Olry, SEP, for valuable discussion.

References

1. Y. HASEGAWA, M. IIMURA and S. YAJIMA, *J. Mater. Sci.* **15** (1980) 720.
2. Y. HASEGAWA and K. OKAMURA, *ibid.* **21** (1986) 321.
3. Y. HASEGAWA, *ibid.* **24** (1989) 1177.
4. K. OKAMURA, *Composites* **18** (2) (1987) 107.
5. T. J. CLARK, R.M. ARONS, I. B. STAMATOFF and J. RABE, *Engng Adv. Sci. Proc.* **7–8** (1985) 576.
6. R. M. SALINGER, T. D. BARNARD, C. T. LI and L. G. MAHONE, *SAMPE Q.* **19/3** (1988) 27.
7. E. BOUILLON, D. MOCAER, J. F. VILLENEUVE, R. PAILLER, R. NASLAIN, M. MONTHIOUX, A. OBERLIN, G. GUIMON and G. P. FIFTZER, *J. Mater. Sci.* **26** (1991) 1517.
8. E. BOUILLON, D. MOCAER, J. F. VILLENEUVE, R. PAILLER and R. NASLAIN, in "Materiaux Composites pour Applications à Hautes Températures", edited by R. Naslain, J. Lamalle and J. L. Zulian (AMAC/CODE, MAC Bordeaux, 1990) p. 15.
9. C. LAFFON, A. M. FLANK, R. HAGEGE, P. OLRY, J. COTTERET, M. LARIDJANI, J. DIXMIER, J. M. MIQUEL, H. HOMMEL and A. P. LEGRAND, *J. Mater. Sci.* **24** (1989) 1503.
10. L. PORTE and A. SARTRE, *ibid.* **24** (1989) 271.
11. T. MAH, N. LECHT, D. E. McCULLUM, J. R. HOENIGMAN, H. M. KIM, A. P. KATZ and H. A. LIPSITT, *ibid.* **19** (1984) 1191.
12. K. OKAMURA, M. SATO, Y. HASEGAWA and T. AMANO, *Chem. Lett.* (1984) 2059.
13. K. OKAMURA, M. SATO and Y. HASEGAWA, "High tech Ceramics", edited by P. Vincenzini (Elsevier Science, Amsterdam, 1987) p. 747.
14. S. YAJIMA, T. IWAI, T. YAMAMIRA, K. OKAMURA and Y. HASEGAWA, *J. Mater. Sci.* **16** (1981) 1349.
15. K. OKAMURA, M. SATO and Y. HASEGAWA, in "Seventh International Conference on Composite Materials (ICCM-VII)", edited by J. Fuller, G. Gruninger, K. Schulte, A. R. Bunsel and A. Massiah (Elsevier Applied Science, London, New York, 1990) p. 573.
16. V. S. R. MURTHY, M. H. LEWIS, M. E. SMITH and R. DUPREE, *Mater. Lett.* **8** (1989) 263.
17. D. B. FISHBACH, P. M. LEMOINE and G. V. YEN, *J. Mater. Sci.* **23** (1988) 987.
18. T. YAMAMURA, T. HURUSHIMA, M. KIMOTO, T. ISHIKAWA and T. IWAI, in "High Tech. Ceramics", edited by Vincenzini (Elsevier Science, Amsterdam, 1987) p. 737.
19. B. G. PENN, F. E. LEDBETTER III, J. M. CLEMONS and J. G. DANIELS, *J. Appl. Polym. Sci.* **27** (1982) 3751.
20. B. G. PENN, J. G. DANIELS, F. E. LEDBETTER III and J. M. CLEMONS, *Polym. Engng. Sci.* **26** (1986) 1191.
21. W. VERBEEK, US Pat. 3853 567 (1974).
22. J. LIPOWITZ, H. AFREEMAN, R. T. CHEN and E. R. PRACK, *Adv. Ceram. Mater.* **2** (2) (1987) 121.
23. G. E. LEGROW, T. F. LIM, J. LIPOWITZ and R. S. REAOCH, *Ceram. Bull.* **66** (1987) 363.
24. H. PORTE and J. J. LEBRUN, Eur. Pat. 0208 630 (1987).
25. G. PEREZ and O. CAIX, in "Fourth European Conference on Composite Materials (ECCM 4) Proceedings", edited by J. Füller, G. Gruninger, K. Schulte, A. R. Bunsell and A. Massiah (Elsevier Applied Science, London, New York, 1990) p. 573.
26. E. BACQUE, J. DUNOGUES, C. BIRAN, P. OLRY and J.P. PILLOT, FR Pat. 2599 037 (1986).
27. D. MOCAER, R. PAILLER, R. NASLAIN, C. RICHARD, J. P. PILLOT and J. DUNOGUES, *J. Mater. Sci.* **28** (1993) 2615.
28. D. MOCAER, R. PAILLER, R. NASLAIN, C. RICHARD, J. P. PILLOT, J. DUNOGUES, C. GERARDIN and C. TAUTELLE, *ibid.* **28** (1993) 2632.
29. Y. MANIETTE and A. OBERLIN, *ibid.* **24** (1989) 3361.
30. P. B. HIRSCH, A. HOWIE, R. B. NICHOLSON, D. W. PASCHLEY and W. J. WHELAN in "Electron Microscopy of thin Crystals" (Butterworths, London, 1975) p. 1.
31. Y. MANIETTE and A. OBERLIN, *J. Mater. Sci.* **24** (1989) 3361.
32. A. R. BUNSELL, J. W. S. HEARLE and R. D. HUTTER, *J. Phys. E Sci. Instrum.* **4** (1971) 868.
33. K. OKAMURA, M. STAO, T. SEGUCHI and S. KAWANISHI, in "Controlled Interphase in Composite Materials", edited by M. Ishida (Elsevier Science, New York, 1990) p. 209.
34. D. LEWIS III, *Ceram. Bull.* **67** (1988) 1349.

35. E. BOUILLON, F. LANGLAIS, R. PAILLER, R. NASLAIN, J. C. SARTOU, A. DELPUECH, C. LAFFON, P. LAGARDE, F. CRUEGE, P. V. HUONG, M. MONTHIOUX and A. OBERLIN, *J. Mater. Sci.* **26** (1991) 1333.
36. Y. HASEGAWA and K. OKAMURA, *ibid.* **18** (1983) 3633.
37. J. J. POUPEAU, D. ABBE and J. JAMET, ONERA Report (1982).
38. A. OBERLIN, in "Chemistry and Physics of Carbon", Vol. 22, edited by P. A. Thrower, (Dekker, New York, Basel 1989) A.
39. T. TAKI, K. OKAMURA and M. SATO, *J. Mater. Sci.* **24** (1989) 1263.
40. M. JAFFE and L. SAWYER, "Ultra Structural Processing of Advanced Ceramic", Vol. 55 (1988) p. 725
41. S. M. JOHNSON, R. D. BRITTAIN, R. H. LAMOREAUX and R. D. ROWCLIFFE, *J. Amer. Ceram. Soc.* **71** (1988) C132.
42. H. FUKUNAGA and K. GODA, in "Progress in Advanced Materials and Process Durability, Reliability and Quality Control", edited by G. Boutelds and R. J. Schliekmann (Elsevier Science, Amsterdam, 1987).

Received 20 July
and accepted 11 August 1992